

Pu(VI) Hydrolysis: Further Evidence for a Dimeric Plutonyl Hydroxide and Contrasts with U(VI) Chemistry

Sean D. Reilly and Mary P. Neu*

Chemistry Division, Los Alamos National Laboratory, Los Alamos, New Mexico 87545

Received October 11, 2005

A significant fraction of plutonium that is soluble in environmental waters and other aqueous solutions can be present as complexes of plutonyl, PuO_2^{2+} . Few thermodynamic data are available for this ion, representing a problematic gap in plutonium chemistry and in the forecasting of radionuclide behavior under contamination and nuclear repository conditions. To address this need and more accurately determine the stoichiometry and stability of the basic hydrolytic products, we completed complimentary potentiometric and spectrophotometric studies of plutonium(VI) hydrolysis over the concentration range of 10^{-2} to 10^{-5} M Pu(VI). Dinuclear hydroxide species $(\text{PuO}_2)_2(\text{OH})_2^{2+}$ and $(\text{PuO}_2)_2(\text{OH})_4^0(\text{aq})$ with hydrolysis constants $\log^* \beta_{2,2} = -7.79 \pm 0.20$ and $\log^* \beta_{4,2} = -19.3 \pm 0.5$ are indicated in all experiments of millimolar Pu(VI), 0.10 M NaNO_3 solutions at 25 °C. At lower Pu(VI) concentrations, at and below 10^{-4} M, the monomeric species PuO_2OH^+ and $\text{PuO}_2(\text{OH})_2^0(\text{aq})$ form with hydrolysis constants of $\log^* \beta_{1,1} = -5.76 \pm 0.07$ and $\log^* \beta_{2,1} = -11.69 \pm 0.05$, respectively. Distinct optical absorbance bands at 842 and 845 nm are reported for the mononuclear and dinuclear first hydrolysis species. Standard hydrolysis constants at zero ionic strength were calculated from the experimentally determined constants using the specific ion interaction theory. The Pu(VI) hydrolysis species and constants are compared with results from previous studies for plutonium and uranium. Major differences between uranyl and plutonyl hydrolysis are described.

Introduction

Plutonium contamination in the environment is of global concern due to nuclear weapons and energy production. The common isotopes of plutonium exhibit chemical and radiological toxicity, high-energy alpha radioactive decay, and extremely long half-lives. Fortunately, plutonium has a low solubility in most aqueous systems at near-neutral pH, existing primarily as tetravalent (hydr)oxides. The small fraction of total plutonium that is soluble often comprises pentavalent and hexavalent molecular complexes and suspended colloids. For example, there is evidence that substantial fractions of soluble plutonium in both marine environments and brines is composed of complexes of hexavalent plutonyl.^{1,2} Complexes of this type tend to have low molecular charges and are expected to have relatively weak adsorptive interactions with minerals compared to other forms of plutonium. These species are therefore considered

to increase the solubility and resulting mobility of plutonium from contamination sources and nuclear repositories.^{3–5} There are few thermodynamic or kinetic data available for plutonyl that would enable the accurate quantitative prediction of plutonium speciation and mobility in environmental waters and under other aqueous conditions. Even the stoichiometry and stability of the fundamental PuO_2^{2+} hydrolysis products are not definitively known.

Because there is little information available on the solution thermodynamics of plutonyl, it is useful to consider the chemistry of the structural analogue uranyl, UO_2^{2+} . Uranium(VI) hydrolysis has been thoroughly studied by a variety of methods, as described in hundreds of reports, and evaluated within the Nuclear Energy Agency chemical thermodynamics project sponsored by the Organization for Economic Cooperation and Development.^{6,7} Uranium(VI) begins to hydrolyze

* To whom correspondence should be addressed. E-mail: mneu@lanl.gov.

- (1) Runde, W.; Reilly, S. D.; Neu, M. P. *Geochim. Cosmochim. Acta* **1999**, *63*, 3443–3449.
- (2) Moore, R. C.; Gasser, M.; Awwad, N.; Holt, K. C.; Salas, F. M.; Hasan, A.; Hasan, M. A.; Zhao, H.; Sanchez, C. A. *J. Radioanal. Nucl. Chem.* **2005**, *263*, 97–101.

- (3) Choppin, G. R. *Radiochim. Acta* **1988**, *43*, 82–83.
- (4) Choppin, G. R.; Wong, P. J. *Aquat. Geochem.* **1998**, *4*, 77–101.
- (5) Silva, R. J.; Nitsche, H. In *Advances in Plutonium Chemistry, 1967–2000*; Hoffman, D. C., Ed.; American Nuclear Society: La Grange Park, IL, 2002; pp 89–117.
- (6) Grenthe, I.; Fuger, J.; Konings, R. J. M.; Lemire, R. J.; Muller, A. B.; Nguyen-Trung, C.; Wanner, H. *Chemical Thermodynamics of Uranium*; North-Holland: Amsterdam, 1992; Vol. 1.

below pH 4 in aqueous 10^{-5} M U(VI) solutions and below pH 3 in 10^{-2} M solutions. The major U(VI) hydrolysis species in these solutions over the pH range 1–9 are polynuclear. UO_2OH^+ is the only mononuclear hydrolysis product present at appreciable concentration up to pH 7 in 10^{-5} M or more concentrated U(VI) solutions. The well-established dinuclear species $(\text{UO}_2)_2(\text{OH})_2^{2+}$ is present over the pH range 3–6 and accounts for at most 40% of the total U(VI) in 10^{-2} M solutions (and less in more dilute uranium solutions). Polynuclear $(\text{UO}_2)_3(\text{OH})_5^+$, $(\text{UO}_2)_4(\text{OH})_7^+$, and $(\text{UO}_2)_3(\text{OH})_7^-$ are the dominant species from pH 5 to 9 in solutions of 10^{-2} to 10^{-5} M U(VI), accounting for up to 100% of the total uranium in solution.

In contrast to uranium(VI), only a handful of publications address the hydrolysis of plutonium(VI).^{7–11} In addition to the increased equipment and precautions required for handling plutonium, experimental Pu(VI) hydrolysis studies are complicated by two aspects of Pu(VI) chemistry. First, the alpha decay of Pu in aqueous solution results in the radiolytic formation of peroxide and radicals, which reduce Pu(VI) over time.¹² The rate of this reduction depends on the Pu isotopic composition and concentration, pH, and nature and concentration of additional species present. Second, as is common for the formation of polynuclear metal–hydroxide species, the rates of Pu(VI) hydrolysis reactions are relatively slow (minutes). Thus, hydrolysis measurements must be made quickly enough to be attributed to pure PuO_2^{2+} and not to lower-oxidation-state plutonium species or radiolysis products, and slowly enough to measure equilibrium concentrations. The result is the caveat that all published Pu(VI) hydrolysis studies involve a system for which equilibrium is not rigorously established. An alternative is to use constants for uranyl species in place of plutonyl in modeling and risk assessment calculations. The data and results described herein illustrate why this approach is inferior.

Most studies of plutonium(VI) hydrolysis have employed the methods of potentiometry, spectroscopy, and analysis of solubility data. Whereas the plutonyl–hydroxide species' stoichiometries differ from study to study, polynuclear species are reported to form and persist independent of the method. Cassol et al. reported pH titrations of 0.10–30 mM Pu(VI) solutions that were interpreted using a hydrolysis model including PuO_2OH^+ , $(\text{PuO}_2)_2(\text{OH})_2^{2+}$, and $(\text{PuO}_2)_3(\text{OH})_5^+$.¹³ Later, Madic et al. reported $(\text{PuO}_2)_2(\text{OH})_2^{2+}$ and $(\text{PuO}_2)_4(\text{OH})_7^+$ in 0.10 M Pu(VI) solutions using Raman spectroscopy.¹⁴ Studies at these higher Pu(VI) concentrations

showed no evidence of a mononuclear first hydrolysis product. In the 1990s, Okajima et al. used conventional visible–near-infrared (vis–NIR) and laser photoacoustic spectroscopies to study the initial hydrolysis of Pu(VI) in the 10^{-2} to 10^{-5} M concentration range. Underscoring the challenges involved in studying plutonium hydrolysis, they first reported the initial hydrolysis product to be PuO_2OH^+ ,¹⁵ and then later concluded that the species was the dinuclear hydroxide $(\text{PuO}_2)_2(\text{OH})_2^{2+}$.¹⁶ Pashalidis et al. used vis–NIR spectra of 10^{-2} to 10^{-3} M Pu(VI) solutions to determine hydrolysis constants for PuO_2OH^+ and $\text{PuO}_2(\text{OH})_2^0(\text{aq})$ in solutions up to pH 5.¹⁷ This study predicted a limited stability range for $\text{PuO}_2(\text{OH})_2^0(\text{aq})$ and the time-dependent formation of polynuclear hydrolysis products above pH 5, on the basis of pH changes over times up to days. In their subsequent study of the solubility of $\text{PuO}_2\text{CO}_3(\text{s})$, PuO_2OH^+ and $\text{PuO}_2(\text{OH})_2^0(\text{aq})$ were identified in vis–NIR spectra of solution fractions.¹⁸

In this study, we use complimentary potentiometric and spectrophotometric techniques to examine plutonium(VI) hydrolysis over the 10^{-2} to 10^{-5} M Pu(VI) concentration range and find major differences from uranium(VI) hydrolysis. We report stepwise hydrolysis of PuO_2^{2+} to produce either mononuclear or dinuclear hydrolysis species, depending on the total Pu(VI) concentration. The instability of Pu(VI) with respect to reduction, coupled with the fact that multiple hydrolytic species exist simultaneously in solution, has thwarted our attempts to obtain confirmatory structural characterization for individual species.¹⁹ Our studies indicate that plutonyl hydrolyzes less readily than uranyl, as expected. In further contrast with U(VI), the major plutonyl polymeric hydrolysis product is a dimer, whereas the predominant U(VI) species under similar conditions is the trimer $(\text{UO}_2)_3(\text{OH})_5^+$.

The values we report for the first Pu(VI) hydrolysis constant compare well with current OECD recommendations.⁷ Optical spectra compare well with previous studies, and an extinction coefficient is reported for the first hydrolysis product. Our data indicate stoichiometry and constants for subsequent hydrolytic species that differ from previous studies. Time-dependent spectroscopic studies suggest that changes in the solution pH and absorbance maxima that were previously attributed to polymerization reactions may in fact correspond to reduction reactions and the related decrease in total Pu(VI) concentration. The species and constants reported here can be considered in future reviews by the OECD and others, used in geochemical fate and

- (7) Guillaumont, R.; Fanghänel, T.; Fuger, J.; Grenthe, I.; Neck, V.; Palmer, D. A.; Rand, M. H. *Update on the Chemical Thermodynamics of Uranium, Neptunium, Plutonium, Americium, and Technetium*; Elsevier: Amsterdam, 2003; Vol. 5.
- (8) Lemire, R. J.; Fuger, J.; Nitsche, H.; Potter, P.; Rand, M. H.; Rydberg, J.; Spahiu, K.; Sullivan, J. C.; Ullman, W. J.; Vitorge, P.; Wanner, H. *Chemical Thermodynamics of Neptunium and Plutonium*; Elsevier: Amsterdam, 2001; Vol. 4.
- (9) Fuger, J. *Radiochim. Acta* **1992**, 58–59, 81–91.
- (10) Fuger, J. *J. Nucl. Mater.* **1993**, 201, 3–14.
- (11) Choppin, G. R. *Radiochim. Acta* **2003**, 91, 645–649.
- (12) Newton, T. W.; Hobart, D. E.; Palmer, P. D. *Radiochim. Acta* **1986**, 39, 139–147.
- (13) Cassol, A.; Magon, L.; Portanova, R.; Tondello, E. *Radiochim. Acta* **1972**, 17, 28–32.

- (14) Madic, C.; Begun, G. M.; Hobart, D. E.; Hahn, R. L. *Inorg. Chem.* **1984**, 23, 1914–1921.
- (15) Okajima, S.; Reed, D. T.; Beitz, J. V.; Sabau, C. A.; Bowers, D. L. *Radiochim. Acta* **1991**, 52–53, 111–117.
- (16) Okajima, S.; Reed, D. T. *Radiochim. Acta* **1993**, 60, 173–184.
- (17) Pashalidis, I.; Kim, J. I.; Lierse, C.; Sullivan, J. C. *Radiochim. Acta* **1993**, 61, 29–34.
- (18) Pashalidis, I.; Kim, J. I.; Ashida, T.; Grenthe, I. *Radiochim. Acta* **1995**, 68, 99–104.
- (19) We found that plutonium hydrolysis samples transported from Los Alamos to the Stanford Synchrotron Radiation Laboratory for X-ray absorbance spectroscopic (XAS) measurements, and therefore subjected to temperature and atmospheric changes, contained precipitates or carbonate complexes and did not yield useful data for this study.

transport models, and applied to experimental designs aimed at structurally characterizing plutonyl species.

Experimental Section

Safety note: Plutonium is radioactive and must be handled with care within laboratories appropriate for research involving transuranic materials. Plutonium solutions other than sealed analytical samples were handled in a chemical fume hood, and dispersible solids were handled in a negative pressure glovebox, both equipped with high-efficiency particulate air (HEPA) filtered exhaust.

Materials. Low carbonate content sodium hydroxide titrant was prepared from concentrate (J. T. Baker) and degassed ultrapure water. The NaOH titrant was standardized against potassium hydrogen phthalate, and the amount of dissolved carbonate remained less than 1%, as determined by Gran's method.^{20,21} Perchloric acid titrant was prepared from reagent grade 70% perchloric acid and degassed ultrapure water and standardized against a base of known concentration. A 0.10 M aqueous sodium nitrate solution was prepared by dissolving this solid in ultrapure water.

Plutonium metal was dissolved in chilled 6 M HCl to give a Pu(III) solution (isotopic composition: 94% ²³⁹Pu; 6% ²⁴⁰Pu; trace ²³⁸Pu, ²⁴¹Pu, and ²⁴²Pu). The Pu(III) solution was mixed with an equal volume of 16 M HNO₃ to give a Pu(IV) solution. The Pu(IV) solution was purified using anion-exchange chromatography as follows: a green Pu(IV) solution in 8 M HNO₃ was loaded onto Bayer Lewatit MP-500 macroporous resin, washed with 8 M HNO₃ followed by 9 M HCl, and then eluted with 0.5 M HCl. Red Pu(IV) stock solutions thus-purified were evaporated under reduced pressure to raise the HCl concentration to 2–4 M, which stabilizes the IV oxidation state. Plutonium(VI) stock solutions were prepared by bubbling ozone through purified Pu(IV) solutions in HCl. The plutonium solution concentration and oxidation state were determined by measuring the vis-NIR spectrum of a solution sample diluted in 1.0 M HClO₄.²² Plutonium(VI) concentration was determined using Beer's Law with the absorbance at 830.5 nm and an experimentally determined molar absorptivity of 538 L mol⁻¹ cm⁻¹.¹ All spectra for quantitative analysis were collected using a Varian Cary 500 spectrophotometer with a fixed spectral bandwidth of 0.2 nm to fully resolve the narrow Pu absorbance bands. Spectra that were used to monitor shifts in absorbance maxima only were collected using an Ocean Optics spectrophotometer. Both instruments were calibrated for wavelength accuracy prior to each experiment.

Potentiometry. All potentiometric equilibrium measurements were conducted on stirred solutions in a water-jacketed vessel at 25.0 ± 0.1 °C under ultrapure argon. The concentration of Pu(VI) in a supporting 0.10 M electrolyte for individual experiments was varied between 10 and 0.10 mM. Titrants were dispensed using a Brinkmann-Metrohm 665 Dosimat autoburet. Potentiometric measurements were made using an Orion Research EA940 pH meter and an Orion ROSS combination pH electrode filled with 3 M aqueous sodium nitrate. The buret and pH meter were interfaced to a personal computer to permit automated data collection using software developed in this laboratory. A pK_w of 13.78 (0.10 M ionic strength NaNO₃, 25 °C) was used in all calculations.²⁰ Combination pH electrodes were calibrated before each titration as follows: To 10 mL of supporting 0.10 M NaNO₃ was added 0.50 mL of standardized 0.10 M HClO₄. Standardized 0.10 M

NaOH was then titrated into the solution in 20 0.05 mL aliquots. The electrode potential was recorded before the titration and after the addition of each aliquot of base. Twenty-one data points were thereby collected over a pH range 2.3–11.4. Linear least-squares analysis of the electrode potential (in mV) as a function of the known acid concentration (below pH 3.0 and above pH 10.5) provided the electrode slope and intercept. This slope and intercept enabled the pH electrode to measure $-\log [H^+]$ (designated p[H]) directly during subsequent titrations of plutonium.

Titrations were performed as follows: A measured volume of ²³⁹Pu(VI) stock solution was added to 5 mL of 0.10 M NaNO₃ and titrated with standardized 0.10 or 0.01 M NaOH while the p[H] was measured. The base aliquot volumes averaged 5–15 μL and were varied throughout the titration in order to keep the pH change between data points relatively constant (0.05–0.25 pH units depending on the Pu concentration). This approach to data collection, variable base addition and regular pH intervals as opposed to the more common approach of constant base addition and variable pH intervals, was used to maximize the number of data points collected in the buffer regions that correspond to speciation changes in solution. The concentration of Pu(VI) was determined by calculating the titration curve derivative, d(titrant volume)/d(p[H]), and assuming that the difference between its two maxima corresponds to 2 equiv of added base titrant. The calculated concentration was within a few percent of the concentration calculated on the basis of the known volume of Pu(VI) stock added. Ten Pu(VI) titrations were performed with a Pu(VI) concentration of 1–10 mM, and an average of 40 data points were collected in a p[H] range of 2.7–8.4 for each data set. Four Pu(VI) titrations were performed with a Pu(VI) concentration of 0.1–0.5 mM, and an average of 50 data points were collected in a p[H] range of 3.7–7.8 for each data set. The data to fitted parameter ratio was therefore approximately 20–25 data points per calculated formation constant for individual stability constant refinements, and approximately 150–200 points were used to calculate each constant considering all of the data points in the study. For each data point, the pH was recorded when the measured pH varied by less than 0.01 pH units over 30 s. Solutions reached this stability criterion within 2–6 min in all of the experiments.

Plutonium(VI) hydrolysis constants ($\log^* \beta$) and associated errors (σ) were determined separately for each set of experimental data using the weighted nonlinear least-squares analysis computer program BETA.^{23,24} The amount of excess acid initially present in each solution (from the addition of highly acidic Pu stock solutions) was varied to produce the best fit to the observed titration curve breakpoint and then fixed in stability constant refinements. A weighted average value of each hydrolysis constant was then calculated using eq 1.

$$\log^* \beta = \frac{\sum_{i=1}^n \{(\log^* \beta)_i / \sigma_i^2\}}{\sum_{i=1}^n \{1 / \sigma_i^2\}} \quad (1)$$

The error reported together with the weighted average $\log^* \beta$ is

(23) Harris, W. R.; Raymond, K. N. *J. Am. Chem. Soc.* **1979**, *101*, 6534–6541.

(24) BETA requires estimates of the intrinsic error in the buret (σ_v) and the pH meter (σ_{meter}). The metal hydrolysis constants reported here were computed using $\sigma_v = 0.015$ mL. The value of σ_{meter} was obtained from electrode calibrations prior to each titration and ranged from 0.005 to 0.058 pH units.

(20) Martell, A. E.; Motekaitis, R. J. *Determination and Use of Stability Constants*, 2nd ed.; VCH Publishers: New York, 1992.

(21) Rossotti, F. J. C.; Rossotti, H. J. *Chem. Educ.* **1965**, *42*, 375–378.

(22) Cohen, D. J. *Inorg. Nucl. Chem.* **1961**, *18*, 211–218.

the standard deviation of the $\log^* \beta_i$ values from individual experiments (experimental errors and errors propagated in the data analysis). Thus, the errors represent the uncertainties in the constants based upon the entire study.

Spectrophotometry. Two methods were employed to collect visible–near-IR spectra of plutonium titration solutions simultaneously with potentiometric data. Titration solution spectra were collected using an Ocean Optics spectrometer configured with a fiber optic dip probe inserted into the titration solution and a detector that is optimal for measuring absorbances in the wavelength range 720–950 nm. The narrow Pu(VI) absorption peaks were not completely resolved by this spectrometer, so these spectra were used only to qualitatively monitor the shift in absorbance maxima and speciation in solution. Titration solution spectra with complete spectral resolution and higher signal-to-noise ratios were collected using a Cary 500 spectrophotometer with a 0.2 nm spectral bandwidth. The potentiometric titration was paused at specific pH values, and an aliquot of the solution was transferred to a 1.0 cm glass cuvette; the spectrum was recorded from 800 to 900 nm. The aliquot was then carefully returned to the titration cell to minimize solution loss during transfers.

Absorbance spectra were also collected from separate experiments in which solutions with 10^{-4} to 10^{-5} M Pu(VI) and pH values of 5.0–9.5 in water or 0.10 M NH_4NO_3 were analyzed as a function of time. Spectra of these dilute solutions were collected using a 10.0 cm path length cell to increase the measured absorbance and signal-to-noise ratio.²⁵ The pH electrode used for these experiments was calibrated using pH 4, 7, and 10 buffers, and the pH measurements were not used in any calculations. (Under these conditions, the solution pH measured with an electrode calibrated using buffers is approximately one unit less than the p[H] measured using an electrode that is calibrated using a standard acid–base titration.)

Results and Discussion

Hydrolysis Constants Determined by Potentiometry.

Plutonium(VI) hydrolysis was studied by titrating acidic 10^{-2} to 10^{-4} M Pu(VI) solutions with a base and fitting the resulting potentiometric curves with possible Pu hydrolysis models. Optical absorbance spectra were collected on the solutions during the course of these titrations to provide independent characterization of the absorption properties and the number of Pu species present in solution. The experimental titration curves exemplified by those shown in Figure 1 exhibit two inflection points, at zero and 2 equiv of added base (based on molar equivalents of plutonyl). The first inflection point corresponds to neutralization of the excess acid in the Pu(VI) stock solution that was added to the titration vessel. The second inflection point at 2 equiv corresponds to the formation of a species with the formula $(\text{PuO}_2)_m(\text{OH})_n^{(2m-n)+}$. Models were refined that both best fit the pH titration data up to 2 equiv of added base and included

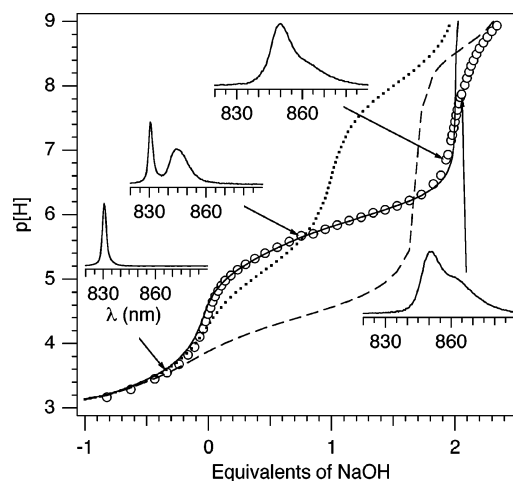
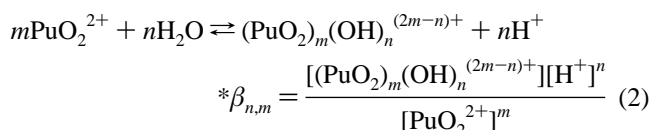


Figure 1. Potentiometric p[H] titration of Pu(VI) with NaOH. Representative near-IR spectra collected during the titration are shown in the insets. Initial Pu(VI) concentration is 1 mM. $I = 0.10$ M NaNO_3 , $t = 25$ °C. Legend: (circles) experimental p[H] data; (solid line) fit; (dotted line) calculated fit using literature Pu(VI) hydrolysis constants (ref 7); (dashed line) calculated fit using literature U(VI) hydrolysis constants (ref 7).

only species consistent with the absorbance spectra. Combinations of potential hydrolysis species used to model the data included mono-, di-, and trinuclear hydrolysis complexes formed in single and multiple proton steps according to reaction 2.



Potentiometric titration data obtained from solutions containing 10^{-2} to 10^{-3} M Pu(VI) were best fit with a model comprising the two species $(\text{PuO}_2)_2(\text{OH})_2^{2+}$ and $(\text{PuO}_2)_2(\text{OH})_4^0(\text{aq})$, with corresponding hydrolysis constants $\log^* \beta_{2,2} = -7.79 \pm 0.20$ and $\log^* \beta_{4,2} = -19.3 \pm 0.5$. Fits were not improved by including monomeric or other polynuclear hydroxide species. Several models that included $(\text{PuO}_2)_3(\text{OH})_5^+$, the analogue of the predominant uranyl hydrolysis species under similar conditions, and known constants for other uranyl species were tested and found to differ significantly from the experimental pH and spectroscopic data. The molar equivalent ratio of plutonium-bound hydroxide to total plutonium, \bar{n} , was calculated from the titration data using eq 3.

$$\bar{n} = \frac{[\text{H}^+] - [\text{H}]_{\text{tot}}}{[\text{Pu}]_{\text{tot}}} \quad (3)$$

In the above equation, $[\text{Pu}]_{\text{tot}}$ is the overall plutonium(VI) concentration in solution, $[\text{H}^+]$ is measured by the pH electrode, and $[\text{H}]_{\text{tot}}$ is the calculated total acid concentration assuming no hydrolysis. Plots of \bar{n} as a function of total plutonium concentration and pH (Figure 2) show that the speciation in the system above 0.5 mM Pu(VI) differs from that at lower concentrations. The higher value of \bar{n} at the same pH for different Pu concentrations confirms the

(25) Overtones of the water vibrational bands are a significant component of the background in the near-IR region of the optical spectrum. The noise contribution associated with these bands scales with the path length. However, instrument noise does not increase with path length so the overall signal-to-noise ratio improves with an increase in path length. The increase in S/N that is gained by using a longer path length cell was separately determined using Nd(III) solutions (described in the Supporting Information). Neodymium(III) was used because it also has narrow and relatively intense absorbance bands in the same region as plutonium(VI), but is easier to handle.

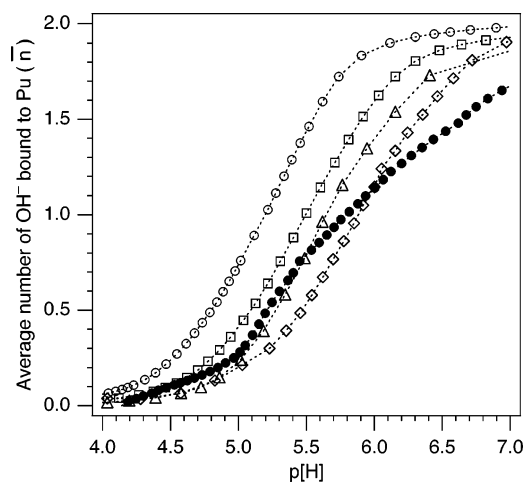


Figure 2. Plot of \bar{n} , the average number of hydroxides bound to plutonyl, as a function of pH and plutonium concentration. Legend: (open circles) 10.0 mM Pu(VI); (open squares) 4.2 mM Pu(VI); (open triangles) 1.0 mM Pu(VI); (open diamonds) 0.5 mM Pu(VI); (filled circles) 0.10 mM Pu(VI).

presence of polymeric species. The same speciation is indicated for all solution experiments conducted with Pu(VI) concentrations ≥ 1 mM. Potentiometric titrations in this concentration range were best fit with the two dinuclear hydrolysis products, $(\text{PuO}_2)_2(\text{OH})_2^{2+}$ and $(\text{PuO}_2)_2(\text{OH})_4^0(\text{aq})$.

Potentiometric and spectrophotometric experiments repeated at lower plutonyl concentrations showed that mononuclear hydrolysis species form in 10^{-4} M solutions. Titration data from these solutions were better fit with a model containing only the monomeric species PuO_2OH^+ and $\text{PuO}_2(\text{OH})_2^0(\text{aq})$. For example, titration data of 0.5 mM and 0.75 mM Pu(VI) are optimally modeled with the two monomeric species, PuO_2OH^+ and $\text{PuO}_2(\text{OH})_2^0(\text{aq})$. (Data collected on a 0.75 mM Pu(VI) solution and fits using mononuclear and dinuclear models are shown in the Supporting Information.) Hydrolysis constants for both the monomeric and dimeric plutonyl species are summarized and compared with corresponding values for uranyl in Table 1.

Spectroscopic Confirmation of the Hydrolysis Model.

Optical spectra collected during potentiometric titrations enabled Pu(VI) hydrolysis to be followed spectrophotometrically as a function of pH and Pu concentration. Representative pH-dependent spectra are shown in Figure 3 for a 1.0 mM Pu(VI) solution. Spectra at low pH show the characteristic intense PuO_2^{2+} aquo ion absorbance at 830 nm. The intensity of this peak, and thus the $\text{PuO}_2^{2+}(\text{aq})$ concentration, decreases with increasing pH as hydrolysis proceeds. PuO_2^{2+} concentrations calculated from these spectra compare well with those calculated from the model generated from the potentiometric data. The initial hydrolysis species at millimolar and higher concentrations, absorbing at 845 nm with a molar absorptivity of $270 \pm 10 \text{ cm}^{-1} \text{ M}^{-1}$, was assigned to be $(\text{PuO}_2)_2(\text{OH})_2^{2+}$ on the basis of correlation with the model determined from potentiometry. By pH 6.85, no Pu(VI) remains unhydrolyzed and a second absorbance band at 850 nm, attributable to $(\text{PuO}_2)_2(\text{OH})_4^0(\text{aq})$, is observed. Further pH increases and Pu(VI) hydrolysis yields an additional absorbance band centered at the higher wavelength

of 864 nm. Potentiometric data in this range are consistent with the formation of $\text{PuO}_2(\text{OH})_3^-$.

Measured spectra of 10^{-4} M Pu(VI) titration solutions are less informative because the absorbances of Pu species at this concentration are near the detection limit of the method. In 0.2 mM Pu(VI) solutions, the first hydrolysis species displays an absorbance maxima at 842 nm (Figure 4, spectrum 1). Results from the modeling of potentiometric data indicate that this is the monomeric species PuO_2OH^+ . Signal-to-noise ratios of spectra of submillimolar Pu(VI) solutions were improved by recollecting spectra using a longer 10 cm path length cell. The spectrum of a pH 7.95, 0.2 mM Pu(VI) solution clearly shows the presence of absorbance bands at 842 and 850 nm (Figure 4, spectra 2–4). The 845 nm absorbance band that is observed in spectra of more concentrated Pu hydrolysis solutions does not appear in spectra of 0.2 mM Pu(VI) solutions. Instead, the absorbance maximum shifts directly to a second maximum at 850 nm.

Changes in pH over longer times (hours to weeks) are common for hydrolysis systems and have been noted for Pu(VI).¹⁷ To consider the effect of time on Pu(VI) hydrolysis, solutions were monitored over the course of several weeks. For example, pH and optical spectra for a 0.2 mM Pu(VI) solution are shown in Figure 4. Spectra and pH for the solution as prepared and after 6 days (Figure 4, spectra 2 and 3) show that the solution pH increased by approximately 0.1 and the ratio of the absorbance at 842 to that at 850 decreased. The total soluble Pu concentration was determined by liquid scintillation counting to have decreased by 11%. These data are all consistent with a slightly reduced soluble Pu(VI) concentration, higher pH, and a corresponding increase in the second hydrolysis species relative to the first. After 13 days, the soluble concentration had further decreased and an absorbance band at 569 nm emerged, which is indicative of Pu(V). Similar Pu(VI) reduction over time has been observed in 10^{-4} M solutions in water at pH 6 and was attributed to radiolytic reduction and the precipitation of Pu in other oxidation states.²⁶ From these studies, we conclude that pH changes over time can be explained by oxidation state changes and effective changes in Pu(VI) concentration and are not necessarily due to further polymerization or agglomeration, as previously reported.¹⁷

Several attempts were made to obtain structural data to confirm the species stoichiometry, including by X-ray absorption spectroscopy. Extended X-ray absorbance fine structure (EXAFS) analysis is generally most accurate for actinide species in solution at millimolar or greater concentrations. Due to the unavoidable time delay and temperature fluctuations between sample preparation in our laboratory, radiological shipment following all Department of Transportation and Los Alamos requirements, and measurement at a synchrotron source, the Pu(VI) hydrolysis solutions changed in solubility and/or composition between preparation and analysis. EXAFS data for millimolar Pu(VI) samples,

(26) Reed, D. T.; Wygmans, D. G.; Aase, S. B.; Banaszak, J. E. *Radiochim. Acta* **1998**, *82*, 109–114.

Table 1. Selected Plutonium(VI)^a and Uranium(VI)^b Hydrolysis Constants

equilibrium ${}^*\beta_{n,m}$	this work		OECD values	
	$\log {}^*\beta^c$	$\log {}^*\beta^d$	Pu(VI) $\log {}^*\beta^e$	U(VI) $\log {}^*\beta^f$
${}^*\beta_{1,1}$	-5.76 ± 0.07	-5.51 ± 0.16	-5.5 ± 0.5	-5.25 ± 0.24
${}^*\beta_{2,1}$	-11.69 ± 0.05	-11.48 ± 0.05	-13.2 ± 1.5	-12.15 ± 0.07
${}^*\beta_{2,2}$	-7.79 ± 0.20	-7.56 ± 0.20	-7.5 ± 1.0	-5.62 ± 0.04
${}^*\beta_{4,2}$	-19.3 ± 0.5	-18.8 ± 0.5		

^a For solutions with a total plutonium concentration greater than 1 mM, the dimer model is more accurate. For lower concentrations, the monomer model and constants should be used. ^b The following additional species are recommended for U(VI), but are not all yet observed in Pu(VI) studies: $\log {}^*\beta_{3,1}^\circ = -20.25 \pm 0.42$, $\log {}^*\beta_{4,1}^\circ = -32.40 \pm 0.68$, $\log {}^*\beta_{1,2}^\circ = -2.7 \pm 1.0$, $\log {}^*\beta_{3,3}^\circ = -11.9 \pm 0.3$, $\log {}^*\beta_{5,3}^\circ = -15.55 \pm 0.12$, $\log {}^*\beta_{7,3}^\circ = -32.2 \pm 0.8$, $\log {}^*\beta_{7,4}^\circ = -21.9 \pm 1.0$. ^c Experimentally determined in this work, $I = 0.10$ M NaNO₃, $t = 25$ °C. ^d Corrected to zero ionic strength using specific ion interaction theory (ref 7, p 709). ^e Ref 7, p 106. ^f Reference 7, pp 64–65.

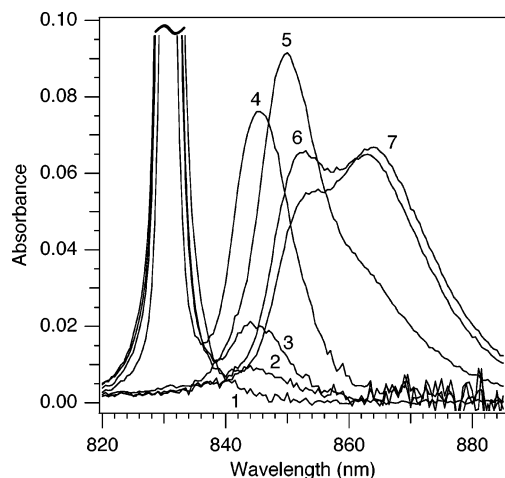


Figure 3. Optical spectra showing progressive Pu(VI) hydrolysis as pH increases during a potentiometric titration. Total Pu(VI) concentration is 1 mM. $I = 0.10$ M NaNO₃, $t = 25$ °C, cell path length = 1 cm. Legend: (1) p[H] 2.26, -4.7 equiv NaOH, $\text{Abs}_{830.5\text{nm}} = 0.542$; (2) p[H] 4.59, 0 equiv NaOH, $\text{Abs}_{830.5\text{nm}} = 0.462$; (3) p[H] 4.90, 0.10 equiv NaOH, $\text{Abs}_{830.5\text{nm}} = 0.416$; (4) p[H] 5.45, 0.55 equiv NaOH, $\text{Abs}_{830.5\text{nm}} = 0.219$; (5) p[H] 6.85, 1.9 equiv NaOH; (6) p[H] 9.48, 2.7 equiv NaOH; (7) p[H] 10.19, 4.2 equiv NaOH.

for which visible inspection of samples prior to measurement suggested the plutonium remained in solution, were consistent with the presence of Pu(VI) carbonate complexes. This change in the speciation is not unexpected given the CO₂ permeability of Kapton and other sample container materials. Results from these studies were equivocal and therefore are not presented here.

Hydrolysis Constants at Standard State Conditions. Specific ion interaction theory (SIT) allows a hydrolysis constant ${}^*\beta_{n,m}$ determined in an ionic medium to be corrected to its value ${}^*\beta_{n,m}^\circ$ at zero ionic strength.⁷ Accordingly, equations (4)–(7) and ${}^*\beta_{n,m}$ determined in 0.10 M NaNO₃ were used to calculate standard state values ${}^*\beta_{n,m}^\circ$ for plutonium(VI) hydrolysis at zero ionic strength.

$$\log {}^*\beta_{1,1} - \Delta z^2 D = \log {}^*\beta_{1,1}^\circ - \Delta \epsilon_{1,1} I_m \quad (4)$$

$$\log {}^*\beta_{2,1} - \Delta z^2 D = \log {}^*\beta_{2,1}^\circ - \Delta \epsilon_{2,1} I_m \quad (5)$$

$$\log {}^*\beta_{2,2} - \Delta z^2 D = \log {}^*\beta_{2,2}^\circ - \Delta \epsilon_{2,2} I_m \quad (6)$$

$$\log {}^*\beta_{4,2} - \Delta z^2 D = \log {}^*\beta_{4,2}^\circ - \Delta \epsilon_{4,2} I_m \quad (7)$$

The density of 0.10 M NaNO₃ used in our experiments is 1.0058 L/kg, and thus its molal ionic strength I_m of 0.10 is

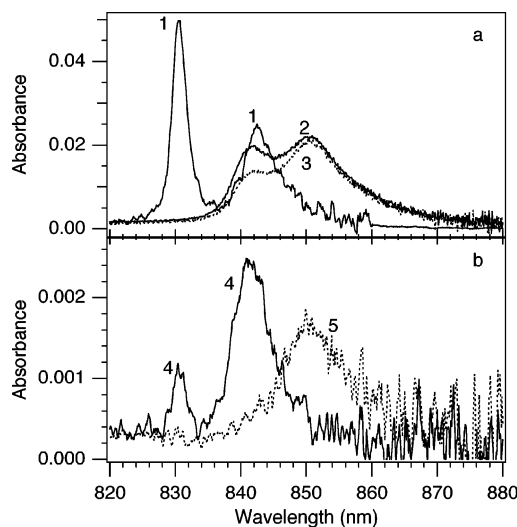


Figure 4. Optical spectra showing initial Pu(VI) hydrolysis species in solutions at (a) 0.2 mM and (b) 0.01 mM total Pu(VI). Legend: (1) p[H] 5.46, 1.0 equiv NaOH, $I = 0.10$ M NaNO₃; (2) spectrum of Pu(VI) in water at time zero, pH 7.92; (3) spectrum of solution (2) after 6 days showing time dependency, pH 8.05; (4) spectrum of Pu(VI) in water at time zero, pH 6.53; (5) spectrum of Pu(VI) in water at time zero, pH 9.47. Spectrum 1 was collected using a 1 cm path length cell. Spectra 2–5 were collected using a 10 cm path length cell and have been smoothed using a 5-point boxcar. (The absorbance spectra shown here have been normalized for path length.)

insignificantly different from its molar concentration. Indeed, $\log {}^*\beta_{n,m}^\circ$ values calculated using molal or molar concentrations differed only in the fourth decimal place, a difference that is insignificant compared to the experimental error. The Debye–Hückel term $D = (0.509 I_m^{1/2}) / (1 + 1.5 I_m^{1/2})$ was calculated to be 0.1092 using 0.10 as the value for I_m . The term Δz^2 is the difference between the sum of the squares of the ion charges of the products and reactants, which is -2 for eqs 4–6 and -4 for eq 7.

Parameters for the ion interaction of cations PuO₂²⁺, PuO₂-OH⁺, and (PuO₂)₂(OH)₂²⁺ with the anion NO₃⁻ are not available. The closest possible analogous uranium(VI) parameters with larger uncertainties were substituted. The same methodology has been used where U(VI) cation interaction parameters with ClO₄⁻ were used for Pu(VI).⁷ Using U(VI) parameters is not ideal given the observed differences in Pu(VI) hydrolysis behavior. However, the interactions between individual actinyl ions and the nitrate ion are smaller and more comparable to each other than interactions between actinyl ions and hydroxide. The alternative substitution of Pu(VI)-ClO₄⁻ interaction parameters

would be less valid, because perchlorate has smaller cation–anion interaction parameters than does nitrate. Hence, the following ion interaction parameters were used: $\Delta\epsilon_{1,1} = \epsilon(\text{UO}_2\text{OH}^+, \text{NO}_3^-) + \epsilon(\text{H}^+, \text{NO}_3^-) - \epsilon(\text{UO}_2^{2+}, \text{NO}_3^-) = 0.34 \pm 1.40$, $\Delta\epsilon_{2,1} = 2\epsilon(\text{H}^+, \text{NO}_3^-) - \epsilon(\text{UO}_2^{2+}, \text{NO}_3^-) = -0.10 \pm 0.04$, $\Delta\epsilon_{2,2} = \epsilon((\text{UO}_2)_2(\text{OH})_2^{2+}, \text{NO}_3^-) + 2\epsilon(\text{H}^+, \text{NO}_3^-) - 2\epsilon(\text{UO}_2^{2+}, \text{NO}_3^-) = 0.15 \pm 0.11$, $\Delta\epsilon_{4,2} = 4\epsilon(\text{H}^+, \text{NO}_3^-) - 2\epsilon(\text{UO}_2^{2+}, \text{NO}_3^-) = -0.20 \pm 0.07$. Ion interaction parameters involving the neutral reaction products $\text{PuO}_2(\text{OH})_2^0(\text{aq})$ and $(\text{PuO}_2)_2(\text{OH})_4^0(\text{aq})$ are zero. The calculated standard state values $^*\beta_{n,m}^\circ$ of the plutonium(VI) hydrolysis species are given in Table 1.

Comparisons of Speciation and Formation Constants with Previous Studies. Constants for monomeric and dimeric plutonium(VI) hydrolysis species determined here are listed in Table 1. Comparable OECD-recommended⁷ values for uranium(VI) and plutonium(VI) are also given. Our value for the first hydrolysis product corrected to zero ionic strength, $^*\beta_{1,1}^\circ$, is within error of the OECD-recommended value and is similar to the value for U(VI). Cassol et al.¹³ and Pashalidis et al.¹⁷ have reported values for $\log ^*\beta_{1,1}$ of -5.97 ± 0.05 and -5.68 ± 0.15 , respectively, in 0.10 M NaClO_4 , which compare reasonably well with the value determined in 0.10 M NaNO_3 .

In contrast, our value for $\log ^*\beta_{2,1}^\circ$ is notably lower than both the OECD value and -13.31 ± 0.18 determined by Pashalidis.¹⁷ Attempts to model the hydrolysis data with either of these values produced poor fits to our observed pH titration and spectrophotometric data. One explanation for the difference is the formation of further hydrolysis species, such as $\text{PuO}_2(\text{OH})_3^-$, with a corresponding formation constant that could be highly correlated with $^*\beta_{2,1}$. The presence of such a species could make the concentration of $\text{PuO}_2(\text{OH})_2^0(\text{aq})$ in solution lower than what our model predicts; the actual value for $\log ^*\beta_{2,1}$ would be more negative than that which we report. A model that included an additional estimated constant of $\log ^*\beta_{3,1}$ of -22 fit the pH titration data well over the entire pH range. Importantly, the addition of this species did not significantly change the calculated value of $\log ^*\beta_{2,1}$. (We note that the value of -22 for $\log ^*\beta_{3,1}$ is an estimate because a precipitate formed at solution pH where this species would be predominant. Use of this constant in thermodynamic data reviews, speciation calculations, and fate and transport modeling is discouraged.)

The corresponding constant for uranyl, $\log ^*\beta_{2,1}^\circ = -12.15$, is greater than expected from a comparison of the first hydrolysis constant for uranyl and plutonyl ($\log ^*\beta_{1,1}^\circ = -5.25$ and -5.51 , respectively). Interestingly, the OECD recommended this constant in part because it is reasonably close to the value for plutonyl. However, the constant was calculated using data from a single indirect extraction study. The new constant for the plutonyl species, $\log ^*\beta_{2,1} = -11.69$, suggests that additional studies are needed to confirm the constant for uranyl.

Okajima et al. reported $\log ^*\beta_{2,2} = -7.3 \pm 0.2$ based on spectroscopic measurements,¹⁶ whereas Cassol's potentiometric data were modeled with $\log ^*\beta_{2,2} = -8.51 \pm 0.05$.¹³ Interestingly, the second dimeric species, $(\text{PuO}_2)_2(\text{OH})_4^0(\text{aq})$,

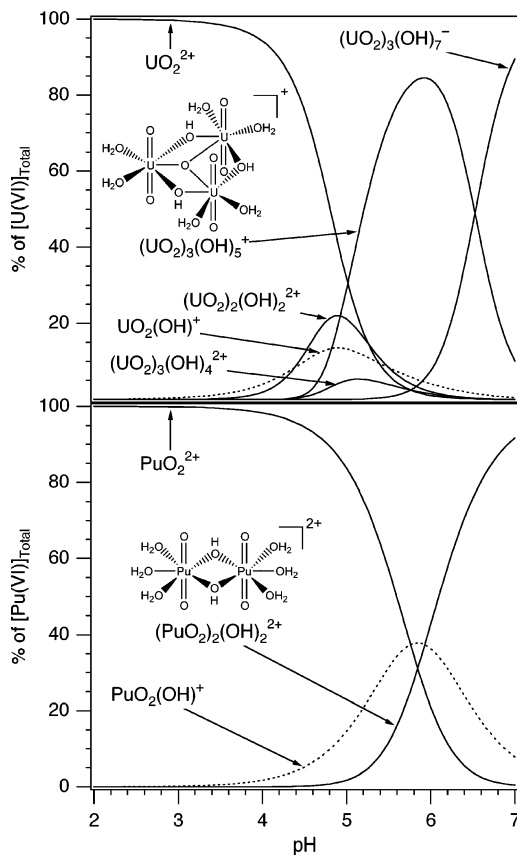


Figure 5. Calculated speciation diagrams for 0.10 mM U(VI) and Pu(VI). The U(VI) diagram is generated using literature constants for U(VI) hydrolysis in 0.10 M NaNO_3 (ref 27). The Pu(VI) diagram is generated using the values for the first monomeric and dimeric hydrolysis constants determined for Pu in 0.10 M NaNO_3 . The monomeric first hydrolysis species of each actinide are accentuated with dotted lines. The known structure of the predominant $(\text{UO}_2)_3(\text{OH})_5^+$ species and the proposed structure of $(\text{PuO}_2)_2(\text{OH})_2^{2+}$ are shown.

has not been previously reported. Although Cassol and co-workers did consider it as a possible species when devising models and observed that a species of the form $(\text{PuO}_2)_m(\text{OH})_{2m}^-$ was indicated by their data that showed \bar{n} reached a value of 2.

Absorbance peaks at 845 and 850 nm observed in optical spectra of millimolar Pu(VI) solutions were assigned to the dimeric species $(\text{PuO}_2)_2(\text{OH})_2^{2+}$ and $(\text{PuO}_2)_2(\text{OH})_4^0(\text{aq})$, respectively (Figure 3). In more dilute Pu(VI) solutions, the monomeric species PuO_2OH^+ and $\text{PuO}_2(\text{OH})_2^0(\text{aq})$ were correlated to absorbances at 842 and 850 nm, respectively (Figure 4). These assignments compare well with those of Pashalidis et al., who found absorbance maxima at 841 and 851 nm and assigned these bands to the mononuclear species PuO_2OH^+ and $\text{PuO}_2(\text{OH})_2^0(\text{aq})$, respectively.¹⁸ By increasing the pH in an initially acidic Pu(VI) solution, they observed an absorption band at 845 nm that shifted toward a higher wavelength of 849 nm with increasing pH. They attributed these bands to the presence of polynuclear species.

Figure 5 shows a comparison of calculated Pu(VI) and U(VI) hydrolysis speciation at 0.10 mM total actinide (An) concentration. The speciation curves for plutonyl were generated using the constants for the monomers listed in Table 1. Those for uranyl are from the most recent

experimental study that was conducted using the same electrolyte and built upon all the past work on uranyl hydrolysis.²⁷ The speciation and titration curves in Figures 1 and 5 show that U(VI) hydrolyzes at a lower pH than does Pu(VI) and that the mononuclear species, PuO_2OH^+ and $\text{PuO}_2(\text{OH})_2^0(\text{aq})$, are more important in 10^{-4} M solutions compared to their U(VI) analogues. In less concentrated 10^{-6} M Pu(VI) solutions, dinuclear species account for less than 5% of the total Pu(VI) concentration, whereas polynuclear species such as $(\text{UO}_2)_3(\text{OH})_5^+$ account for as much as 70% of the total U(VI).

Conclusions

Plutonium solution behavior at very low plutonium concentration, e.g., under conditions appropriately used in reactive transport models and in far-field nuclear waste repository risk assessments, is more accurately described by these new refined complex formation constants than by extrapolating from known uranyl hydrolysis constants, neglecting Pu(VI) species, or using less accurate and/or precise constants. For systems in which the total plutonium concentration is below 10^{-4} M, the mononuclear species and constants are applicable; for ≥ 1 mM plutonium, the dimeric model is more accurate.

We find no evidence for other polynuclear hydroxides such as $(\text{PuO}_2)_3(\text{OH})_5^+$ and $(\text{PuO}_2)_4(\text{OH})_7^+$, analogues of the species that dominate uranium(VI) hydrolysis at uranium concentrations above 10^{-7} M. The onset of U(VI) hydrolysis at pH lower than that for Pu(VI) and the stability of the trimeric $(\text{UO}_2)_3(\text{OH})_5^+$ species reflects the greater oxophilicity of U(VI) compared to Pu(VI). It is noteworthy that

plutonyl is more soluble than uranyl, particularly in solutions containing sodium salts, consistent with different speciation. Precipitates that are most likely due to the formation of $\text{PuO}_2(\text{OH})_2^0(\text{s})$ were not observed below pH 8 in any of the 10^{-5} to 10^{-2} M Pu(VI) solutions. In a broader context, the hydrolysis onset pH difference is consistent with the "harder" nature of U(VI) relative to Pu(VI), as reflected in the formation constants of their respective fluoride complexes: $\log^* \beta_{1,1}^{\circ}$ for the formation of AnO_2F^+ is 4.56 ± 0.20 for Pu(VI) and 5.16 ± 0.06 for U(VI). Although much has been made of the similarity of actinyl ions, the disparity in hydrolysis chemistry demonstrates that there is no direct chemical analogue for Pu(VI). The complicated nature of the plutonyl hydrolysis emphasizes the need for continuing research, particularly validation of the compositions of solution species by structural characterization and molecular detection methods.

Acknowledgment. This work was sponsored by the Heavy Element Research Program, Chemical Sciences Division of the Office of Basic Energy Sciences, and the Environmental Management Science Program, Office of Biological and Environmental Research, U.S. Department of Energy Office of Science. Los Alamos National Laboratory is operated by the University of California for the U.S. Department of Energy under Contract W-7405-ENG-36.

Supporting Information Available: Figure of an experimental titration curve of a 0.75 mM Pu(VI) solution fit with either a monomeric or polymeric model; figure showing the effect of cell path length on signal-to-noise in the NIR region used to study plutonyl hydrolysis. This material is available free of charge via the Internet at <http://pubs.acs.org>.

(27) De Stefano, C.; Gianguzza, A.; Leggio, T.; Sammartano, S. *J. Chem. Eng. Data* **2002**, *47*, 533–538.

IC051760J